Journal of Mathematical Chemistry 4(1990)271–293

STRONGLY CORRELATED ELECTRONIC GROUND STATES IN METALS NEAR THE METAL–INSULATOR TRANSITION

N.H. MARCH
Theoretical Chemistry Department, University of Oxford, 5 South Parks Road, Oxford OX1 3UB, UK

Abstract

The model in which positive ions in a metal are smeared into a uniform neutralizing background in which interacting electrons move is first considered at some length, especially rather near to the metal–insulator (Wigner) transition. Properties considered carefully are (a) the electronic momentum distribution as a function of background density, and (b) the pair correlation function. Features connected with both the long-range Coulombic repulsion and the transition from delocalized to localized behaviour will be highlighted in terms of (a) and (b) above. The possible use of this model as a reference state against which to consider the alkali metals, in both normal and expanded form, will then be discussed. In Na, the importance of 3s–3p hybridization will be emphasized, the Heisenberg model providing a surprisingly useful account of some bulk properties. Diffraction evidence on the degenerate electron assembly in molten Na and K will be considered in support of pronounced metallic bonding. Expanded Cs along the coexistence curve will next be treated, especially the observed magnetic susceptibility which changes from Fermi liquid behaviour to Curie–Weiss form as the critical point is approached. The crossover point is discussed in terms of heavy fermion theory and is shown to contain information about the discontinuity of the electronic momentum distribution at the Fermi surface. This discontinuity is much smaller than that in jellium (the smeared ion model above) and testifies to the importance of the electron–ion interaction at this density, which cannot be treated perturbatively. Finally, the possibility of the co-existence of molecules in metallic phases is considered, with particular reference to metallic hydrogen and metallic iodine near the metal–insulator transition. For the latter, experimental evidence can leave little doubt that there is at least a limited range of pressures over which the metallic ground state of iodine contains I_2 molecules, and some discussion of this strongly correlated state will be included.

1. Introduction

Progress in the treatment of electron correlation in initially metallic systems has come from a variety of directions. Two classes of approach are worth distinguishing at this point:

(1) Treatments which include a full account of the long-range Coulombic repulsion e^2/r_{ij} between electrons i and j at separation r_{ij} (see particularly section 2); and

(2) treatments based on the Hubbard Hamiltonian, in which attention is focused on the intrasite repulsion energy U which acts to prevent two electrons with opposed spins coming on to the same site (see particularly section 4.4).

It is true to say that use of the full interaction e^2/r_{ij} has been mainly restricted so far, in quantitative work, to the so-called jellium model defined below and to metallic hydrogen. In the former, the positive ions in the metal (e.g. Na) are smeared out into a uniform neutralizing unresponsive background in which electrons interacting via e^2/r_{ij} move. All important then, in discussing the role of electronic correlations in the jellium model, is the mean interelectronic spacing r_s, defined in terms of the uniform electron density, ρ_0 say, by

$$\rho_0 = 3/4\pi r_s^3. \tag{1.1}$$

In simple metals, e.g. Al or Na, r_s varies from $2-5.5a_0$, where $a_0 = \hbar^2/me^2$ is the Bohr radius.

For many purposes, the properties of this model can be usefully characterized by:

(1) The electronic momentum distribution $n(p)$, which is, of course, a function of the interelectronic spacing r_s, with $n(p)$ most fundamentally defined from the first-order density matrix $\gamma(\boldsymbol{r}_1, \boldsymbol{r}_2)$ through

$$\gamma(\boldsymbol{r}_1, \boldsymbol{r}_2) = \sum_{\boldsymbol{p}} n(p) \exp(\mathrm{i}\boldsymbol{p} \cdot (\boldsymbol{r}_1 - \boldsymbol{r}_2)/\hbar), \tag{1.2}$$

and

(2) the electronic pair function $g(\boldsymbol{r}_1, \boldsymbol{r}_2) \equiv g(r): r = |\boldsymbol{r}_1 - \boldsymbol{r}_2|$, where in essence $g(\boldsymbol{r}_1, \boldsymbol{r}_2)$ is the diagonal element of the second-order density matrix.

These quantities $n(p)$ and $g(r)$ will be discussed in section 2 below: they will also provide a "reference" system for the fluid alkali metals to be treated in section 3.

Since much emphasis will be placed on the role of directional bonding in the correlated systems discussed in sections 3–5, it is here worth referring to the work of Coulson and Fischer [1] on the free space H_2 molecule. These workers were interested, essentially, in the range of validity of the delocalized "molecular orbital" theory of this simplest molecule. To examine this point, they constructed asymmetric orbitals $\psi_a + \lambda\psi_b$, $\lambda \leq 1$, to be centered on proton a, and $\psi_b + \lambda\psi_a$ to be placed on nucleus b. With the (space only) variational trial function

$$\Psi_{\text{Coulson–Fischer}}(\boldsymbol{r}_1, \boldsymbol{r}_2, R) = [\psi_a(\boldsymbol{r}_1) + \lambda(R)\psi_b(\boldsymbol{r}_1)][\psi_b(\boldsymbol{r}_2) + \lambda(R)\psi_a(\boldsymbol{r}_2)], \tag{1.3}$$

these workers calculated $\lambda(R)$ variationally for a range of internuclear separations R. Their remarkable finding was that, over the range $0 < R < 1.6\,R_{\text{equil}}$, $\lambda(R)$ was identically equal to unity, but that for larger R, λ rapidly decreased to zero with

increasing R. Roughly speaking, as the nuclei were separated by more than 1.6 R_{equil}, electron correlation was "driving electrons back on to their own atoms"; that is, a localized picture then affords the appropriate description. The counterpart of the Coulson–Fischer treatment in solids was supplied independently by Gutzwiller [2], whose work will again be referred to below.

2. Jellium model near Wigner transition

Because of the kinetic energy operator involving ∇^2, the kinetic energy per electron scales as $1/r_s^2$, whereas the Coulomb potential energy scales as $1/r_s$. Thus, in the extreme high density limit, r_s tends to zero, all momentum space is filled with paired spin electrons out to the Fermi sphere radius $p_f = \hbar k_f$ with p_f the Fermi momentum and k_f the corresponding wave number. All higher momentum states are unoccupied and hence $n(p) = 1$ for $p \leq p_f$ and is zero for $p > p_f$. Now consider the other, low density, limit in which r_s tends to infinity. As Wigner [3] recognized more than fifty years ago, the potential energy will now dominate and the electrons will take up a configuration to make this potential energy a minimum. To do this, they must seek to avoid each other optimally, and Wigner recognized that they would do so by localizing on a lattice: the so-called Wigner electron crystal. Then the energy per electron is, as r_s tends to infinity, simply the Madelung energy of point electrons on the lattice sites embedded in the uniform neutralizing background. The lowest energy turns out to correspond to a body-centered-cubic (bcc) structure, the potential energy per electron being given by

$$E = -\frac{1.8}{r_s}, \tag{2.1}$$

where this formula gives the energy in Rydbergs if r_s is in atomic units. This is to be compared with the exchange energy per electron due to the Fermi hole (see eq. (2.3) below) of $-0.916/r_s$. Corresponding to the energy per particle in the low density limit, which is all potential, the kinetic energy per electron in the high density limit is given by

$$E = \frac{2.2}{r_s^2}. \tag{2.2}$$

It is interesting that, after much theoretical study reviewed by Singwi and Tosi [4], the computer simulation work of Ceperley and Alder [5] has settled the critical value of r_s, say r_c, at which the transition from delocalized electron liquid to Wigner crystal occurs at about $100a_0$, with a possible error of $\pm 20a_0$. Herman and March [6] have subsequently noted that an extension of eq. (2.1) to allow for electrons to vibrate about the lattice sites of the Wigner crystal allows a useful representation of the ground-state energy of jellium for quite a range of r_s on either side of the metal–insulator transition.

2.1. MOMENTUM DISTRIBUTION FUNCTION AND PAIR CORRELATIONS

After this brief discussion of the ground-state energy, let us turn to consider both $n(p)$ and the corresponding electron pair function $g(r)$ as r_s is increased from the free Fermi gas limit, where it tends to zero. Then, for a long time it has been known that the effect of interelectronic interactions is to raise the kinetic energy by promoting some electrons outside the Fermi surface radius p_f and thereby leaving holes inside. This creation of electron–hole pairs is a basic many-body effect leading to so-called correlation kinetic energy (see, for example, ref. [7]), but in turn reducing the potential energy favourably and hence leading to a lower energy than the single Slater determinant of plane waves. The schematic form of $n(p)$ is shown in fig. 1, compared with the

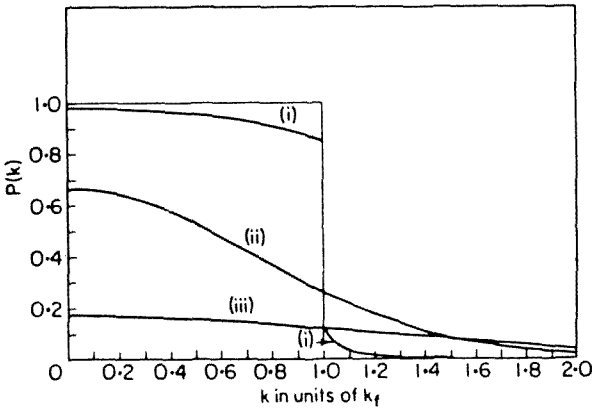

Fig. 1. Shows probability $P(k)$, equivalent to momentum distribution $n(p)$, with $p = \hbar k$, as a function of k in units of Fermi wave number k_f. Curves labelled (i) are for small r_s. Curve labelled (ii) is Gaussian form characteristic of Wigner insulating crystals, where discontinuity q has gone to zero. Curve (iii) represents an even lower density (larger r_s) in the insulating phase. It should be noted that the rectangular Fermi distribution, $P(k) = 1$ for $k \leq k_f$ and zero otherwise, characteristic of limit r_s tends to zero, and gives rise to curve (i) as the Coulomb repulsions are switched on, the part of (i) outside k_f being due to promotion of electrons outside the Fermi sphere, leaving some holes inside.

Fermi gas step function with unit discontinuity at the Fermi surface. March et al. [8] have employed the discontinuity $q(r_s)$ depicted in fig. 1 as an order parameter in a phenomenological theory of the metal–insulator transition in the ground state. This discontinuity q will be of considerable importance for what follows.

One immediate consequence of non-zero q in the metallic phase is that it is reflected in the long-range behaviour of the off-diagonal density matrix γ. Thus, returning to eq. (1.2), Fourier transform theory makes it plain that such behaviour is dominated by the non-analytic points in $n(p)$. Specifically (see below for free electrons), γ falls off at large separation $|r_1 - r_2| = r$ say, as $\cos k_f r / r^2$. As $q(r_s)$ decreases on

approaching the metal–insulator transition, so will the amplitude of such an oscillatory term decrease proportionately. Once in the insulating phase, the off-diagonal elements can be expected to decay exponentially at large r. These statements are easily verified by considering the examples of (a) free electrons, and (b) highly localized Wigner electrons. For (a), appeal to eq. (2.3) below which, together with the asymptotic property $j_1(x) \sim \cos x/x$ at large x of the first-order spherical Bessel function, confirms the metallic behaviour already quoted. As for the Wigner crystal in the limit of very large r_s, use of the Wigner Gaussian orbital leads immediately to $\gamma(r) \sim \exp(-\alpha r^2/4)$, where $\alpha = r_s^{-3/2}$, confirming the limit referred to in the insulator.

Turning from these consequences of the behaviour of the momentum distribution $n(p)$ to the pair function $g(r)$, this is readily calculated – as first shown by Wigner and Seitz [9] – from the single Slater determinant of plane waves valid as r_s tends to zero:

$$g(r) = 1 - \frac{9}{2}\left\{\frac{j_1(k_f r)}{k_f r}\right\}^2 \; ; \quad r_s \text{ tends to zero,} \tag{2.3}$$

representing the so-called Fermi or exchange hole, due to the Pauli principle correlations between parallel spin electrons. The zero-distance correlation $g(r = 0)$ is then 1/2 in this limit for the perfectly paired paramagnetic state described by eq. (2.3).

As was pointed out by Gaskell et al. [10], the large r limit of $g(r)$ in eq. (2.3), which is given by replacing $j_1(x)$ by its large x form, can be interpreted as follows. Using the double angle formula for $\cos^2 x$ in this large r form of $g(r)$ then allows the asymptotic form of $g(r) - 1$ to be written as a sum of two pieces: one proportional to $1/r^4$ coming from the non-analytic point in k space at $k = 0$ (see eq. (2.4) below), and the other, proportional to $\cos(2k_f r)/r^4$ from the second singular point of eq. (2.4) at $2k_f$.

As studied recently by Holas and March [11], the decay of the piece coming from $k = 0$ is changed strongly by incorporating the long-range Coulomb correlations into eq. (2.3), leading from the r^{-4} decay of the Fermi hole to a more rapid fall-off as r^{-8} in the correlated electron liquid. Although the piece coming from the Fermi sphere diameter $2k_f$ is reduced in amplitude essentially because of the reduction in the discontinuity $q(r_s)$ in $n(p)$ with increasing r_s, this contribution turns out away from $r_s = 0$ to dominate the long-range behaviour of the pair function in the electron liquid. Specifically, the leading Fermi hole term $\cos(2k_f r)/r^4$ is multiplied by 1 plus a first-order correction which has a weak r dependence of the form $(\gamma + \ln(2r))^3$. Using $x \equiv 1 - \exp(-x)$, Holas and March [11] note that this could lead to a form $[1 - (r_0/r)^{\mu}]^2$, which could herald a term which modifies the long-range behaviour slightly; namely, by a fractional (μ) increase in the power of r, where μ has the form $(\alpha r_s/2\pi)^{1/2}$ while $r_0 = (2\exp\gamma)^{-1} \equiv 0.3$, with γ equal to Euler's constant.

It is worth expressing the above results directly in k space by writing the electronic structure factor $S(k)$. This is defined such that $S(k) - 1$ is the Fourier transform of $g(r) - 1$. From eq. (2.3) it follows that the Fermi hole in k space has the closed form

$$S(k) = a_1 k + a_3 k^3, \qquad k \leq 2k_f;$$
$$= 1 \qquad\qquad k > 2k_f, \tag{2.4}$$

where $a_1 = 3/4k_f$ and $a_3 = -1/16k_f^3$. The term in r^{-4} in $g(r) - 1$ at large r arises from the k term at small k, as already mentioned. The low-order derivatives of $S(k)$ are evidently discontinuous at the diameter of the Fermi sphere $2k_f$, and this yields a leading term from this singular point proportional to $\cos(2k_f r)/r^4$ in $g(r) - 1$ at large r.

The work of Holas and March [11] has pressed this point of view using many-body techniques in the interacting electron liquid. Their work establishes the small k expansion of $S(k)$ in the presence of Coulombic repulsions as

$$S(k) = a_2 k^2 + a_4 k^4 + a_5 k^5 + \ldots , \tag{2.5}$$

this work being motivated by earlier work of the present author [12] on the π-electron liquid in polyacetylene, where it was proposed that in this one-dimensional case, $S(k)$ had its leading non-analyticity at $O(k^3)$. Both this one-dimensional result and eq. (2.5) have then consequences for the dispersion of the collective electron density oscillations. In fact, as discussed for instance in the book by March and Tosi [13], the term k in the Fermi hole form (2.4) is precisely cancelled because the long-range Coulomb repulsion between electrons leads to such organized electron density oscillations with known frequency ω_p. In turn, the Ornstein–Zernike direct correlation function $c(r)$, when defined in k space just as for a classical liquid by $c(k) = (S(k) - 1)/S(k)$, behaves as $(e^2/r)/(\frac{1}{2}\hbar\omega_p)$ (cf. the classical result $-\phi(r)/k_B T$, with $\phi(r)$ the pair potential), $\frac{1}{2}\hbar\omega_p$ being the zero-point energy of the electron density oscillations. This results in the leading term of $S(k)$ at small k as in eq. (2.5), the coefficient a_2 being precisely $\hbar/2m\omega_p$.

Having discussed the large r form of $g(r)$, it is of some interest to turn to a brief discussion of the small r behaviour.

2.2. POSITIVE DEFINITE PAIR FUNCTION; IN PARTICULAR $g(r = 0) \geq 0$

Most theories of the pair function $g(r)$ in jellium in the electron liquid phase have difficulties for sufficiently large r_s with the condition that $g(r) \geq 0$. This condition is particularly taxing for approximate theory at $r = 0$.

While not perhaps having, to date, the sophistication of established theories such as STLS (see Singwi and Tosi [4]), Dawson and March [14] have proposed an approximate way of incorporating interactions, starting from the Fermi hole (2.3) as the unperturbed state. These workers note that this pair function for non-interacting fermions can be expressed in terms of the density of the p component in the free-electron density matrix. This motivates the treatment of the Coulomb repulsion via a potential energy $V(r)$. To close this theory, one may then invoke self-consistency to determine $V(r)$.

This approach has been examined numerically by Schinner [15], who draws rather optimistic conclusions about the potentiality of the method for large r_s. In particular, in his calculations he finds that the zero-range correlation $g(0, r_s)$ remains positive over the range of r_s that he considers.

While concerned with $g(0, r_s)$, it is relevant to note here that in the localized electron crystal regime, the electronic pair function at $r = 0$ must be very small. Then, the argument used by Bhatia and March [16] for classical liquids leads to an approximate relation between the position, k_m say, of the principal peak of the electronic structure factor $S(k)$ and the peak width $2\Delta k$. Precisely, $2\Delta k$ represents the distance between the two adjacent nodes of $S(k) - 1$ which embrace k_m. Specifically, one finds

$$S(k_m) k_m^2 \Delta k \cong \tfrac{1}{3} k_m^3 \left[1 - \frac{9\pi}{2} \frac{1}{(r_s k_m)^3} \right]. \tag{2.6}$$

Whether this also holds, to a useful approximation, in the metallic electron liquid phase is a matter requiring further investigation.

Density matrix near its diagonal

Earlier, in connection with the discontinuity q in $n(p)$ in the metallic phase, the behaviour of the first-order density matrix $\gamma(r)$ far from the diagonal was examined. Here, it is of interest to note that the form of $\gamma(|\mathbf{r}_1 - \mathbf{r}_2|) \equiv \gamma(r)$ for jellium near the diagonal involves $g(0, r_s)$ in a clear-cut manner. Using the results of Kimball [17] for $n(p)$ at large p, the present author [18] has noted that for small r the expansion of γ around the diagonal density has the form

$$\gamma(r) = \rho_0 + \gamma_2 r^2 + \gamma_4 r^4 + \gamma_5 r^5 + \ldots . \tag{2.7}$$

The point to be emphasized here is the appearance of the non-analytic term in r^5, which has its origin in the fact that $n(p)$ falls off at large p as p^{-8}. Kimball [17] showed that the magnitude of this term, which appears to first have been identified by Daniel and Vosko [19], depends on $g(0, r_s)$, the value of the coefficient of r^5 being recorded in the work of the present author [18]. It is clear that this term is very small, if not zero, in the Wigner electron crystal, as follows from the pair function calculations by March and Young [20] in the insulating phase.

3. Normal and expanded alkali metals

For a long time, it seemed that the alkali metals were almost ideal "nearly-free electron" crystals and that the jellium model of section 2 might therefore be appropriate to describe their conduction electrons. However, even if that were true, there is no escaping the fact that the alkalis Na, K, and especially Cs to be discussed also at some

length below, are low electron density materials, r_s for Cs being $5.5a_0$ – the largest value for all the s–p metals.

Thus, it should occasion no surprise that electron–electron correlations are strong in the alkali metals. What is more surprising is the evidence that is now building up which shows that, in treating these strong interelectronic repulsions quantitatively, the electron–ion interaction has also to be treated carefully. Below, this will first be illustrated by summarizing work on crystalline Na [21] in which quantum-chemical knowledge of the Na_2 molecule is explicitly used. This already testifies to the importance of hybridization in metallic Na, and this point of view will be bolstered by citing and interpreting diffraction evidence [22] pertaining to the conduction electron liquid in molten Na [23] and K [24].

3.1. SOLID Na: HEISENBERG MODEL CHARACTERIZED BY DIATOM POTENTIAL CURVES

For the alkali metals, Malrieu et al. [21] have constructed an effective Heisenberg Hamiltonian from diatom potential curves following the lead of Poshusta and Klein [25] on hydrogen. After illustrating its qualitative validity on small clusters, these workers then considered its solutions for metallic Na, in particular, in various crystal structures, their results for body-centered-cubic (bcc) and simple cubic (sc) lattices being utilized below. Their procedure consisted of considering one of the most ordered spin distributions and, by perturbation due to coupling, with less-ordered spin distributions.

For later purposes, let us note first that the Heisenberg Hamiltonian for Na metal in particular [21] was characterized by the $^1\Sigma_g^+$ and $^3\Sigma_u^+$ potential curves of the free-space diatom Na_2. Then, defining [21] two functions R and g through

$$R(r) = E(^3\Sigma_u^+); \quad g(r) = [E(^3\Sigma_u^+) - E(^1\Sigma_g^+)]/2, \tag{3.1}$$

the resulting Hamiltonian was used to calculate the energy as a function of near-neighbour distance r for both bcc and sc structures. The results may be summarized as follows:

$$E_{bcc}(r) = 4R(r) + 3R\left(\frac{2}{\sqrt{3}}r\right) - 4g(r)[1 + f(r) - 15f^3(r)], \tag{3.2}$$

where

$$f_{bcc}(r) = \frac{g(r)}{14g(r) - 12g\left(\frac{2}{\sqrt{3}}r\right)}, \tag{3.3}$$

while

$$E_{sc}(r) = 3R(r) + 4R\left(\sqrt{2}r\right) - 3g(r)[1 + f(r) - 11f^3(r)], \tag{3.4}$$

with

$$f_{sc}(r) = g(r)/\left[10g(r) - 16g\left(\sqrt{2}r\right)\right]. \tag{3.5}$$

To illustrate the success of this approach to the calculation of thermodynamic properties of crystalline metallic Na in the bcc phase, table 1 collects, for lattice parameters, cohesive energy and bulk modulus, theoretical and experimental values; there is good agreement. An additional point worth making in the present context is that the close-packed face-centered cubic (fcc) and hexagonal-close-packed (hcp) structures turn out to be nearly degenerate, which may afford an explanation of the low-temperature martensitic transformation [21].

Table 1

Structural properties of sodium

	r_e (a.u.)	E_{coh} (eV)	Bulk modulus ($\times 10^{12}$ dyn/cm^2)
bcc			
Order 0	7.18	1.06	0.053
Calc. order 2	6.97	1.253	0.065
Calc. order 4	7.07	1.191	0.065
Expt.	6.99	1.113	0.068
hcp or fcc			
Order 0	7.35	0.993	
Calc. order 2	6.18	1.34	
Calc. order 4	7.20	1.164	
Expt.	7.19	≈ 1.11	
Cubic			
Order 0	7.02	0.866	
Calc. order 2	6.61	1.020	
Calc. order 4	6.82	1.015	

From this evidence supporting the utility of the chemical bonding description of crystalline Na, let us turn to the closely related problem of the way in which electrons correlate when the ions have only short-range order, as in liquid Na and K, following the idea of Egelstaff et al. [22].

3.2. DIFFRACTION EVIDENCE FOR VALENCE BONDING IN LIQUID Na

Egelstaff et al. [22] pointed out that the three partial structure factors required to characterize two-component liquid metals, say Na^+ ions and electrons (e^-), namely $S_{ion-ion}(k) = S(k)$, $S_{electron-ion}(k) = S_{ei}(k)$ and $S_{electron-electron}(k) = S_{ee}(k)$ are in fact accessible experimentally. Thus, $S(k)$ can be determined directly from neutron scattering off the ionic nuclei, while $S_{ei}(k)$ and $S_{ee}(k)$ both enter the expressions for X-ray and electron scattering. So far, experimental difficulties with electron scattering have precluded a full analysis, but this area remains of considerable interest as discussed, for

example, by Chihara [26] and by Tamaki [27]. The idea that the range of order implicit in $S_{ee}(k)$ was different from the short-range order of the ions, proposed in ref. [22] by comparison solely of X-ray and neutron data at the principal peak of $S(k)$, was pressed at other k values by Dobson [23] for Na and subsequently by Johnson [24] for K. Their conclusion was the same; the difference data indicated "diffraction" peaks consistent with electronic short- and medium-range order as in an fcc lattice. Subsequently, March and Tosi [28] proposed a quasi-lattice model to interpret the data; this is shown in fig. 2. To break the bcc-like order of the ions, corresponding to measured coordination number $z = 8$ in the liquid at melting temperature, sp^3 hybridization was invoked,

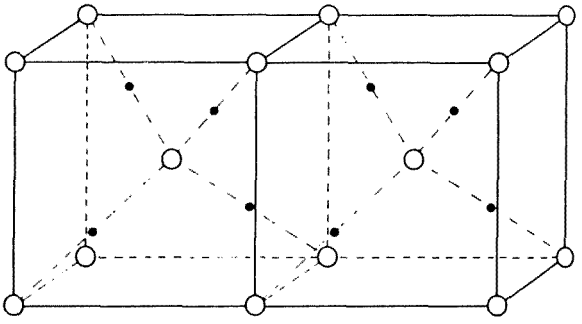

Fig. 2. Depicts the bond model proposed by March and Tosi [28] to explain the difference between neutron and X-ray diffraction data from liquid Na and K just above their melting points. Alkali metal ions are indicated by open circles, their coordination number being $z = 8$ as in a body-centered cubic lattice. Dots show electron "bond charge" centers on bonds joining the ion at the body center to four near neighbours in a tetrahedral configuration. Resonance of the "unoccupied" bonds to the remaining four corners of the cube from the body center is implied.

the electrons having considerable wave amplitude at the bond centers. Pauling-type resonance was then invoked to yield the picture shown in fig. 2, which is consistent with experimental diffraction data. Related evidence for strong spatial electronic correlation in expanded fluid Cs will be presented in the following section.

3.3. PROPERTIES OF EXPANDED FLUID Cs

3.3.1. Electronic momentum distribution and magnetism in metallic Cs

Chapman and March [29] have applied heavy fermion theory in order to interpret the behaviour of the magnetic susceptibility of Cs as measured along the coexistence curve by Freyland [30]; see also Warren [31]. As can be seen in fig. 3, there is a crossover from Fermi liquid to Curie–Weiss behaviour as one moves up the coexistence curve toward the critical point. Although, of course, there is also ionic disorder in such

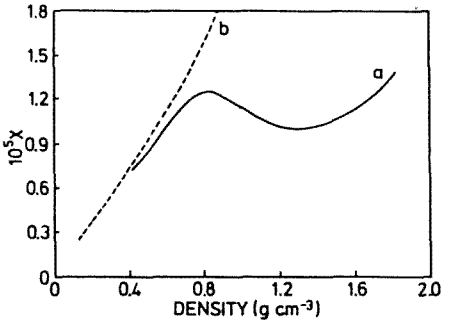

Fig. 3. Magnetic susceptibility versus density of liquid Cs along the liquid–vapour coexistence curve. Experiments by Freyland [30] are shown in the solid curve a. The broken line b, following Warren [31], depicts free-spin Curie susceptibility constructed for densities and temperatures along the coexistence curve.

expanded alkali metals, Chapman and March make the plausible assumption that it is the increasing role of electron correlation as the density is lowered that causes the "crossover" between the types of magnetic behaviour referred to above. While Chapman and March develop both a phenomenological theory using the earlier work of ref. [8] as a starting point, with the discontinuity q, say, in the electronic momentum distribution as the order parameter of the treatment of the metal–insulator transition, and a microscopic approach using the work of Rice et al. [32], it is important to note here that the condition for "crossover" takes the form

$$k_B T_{\text{crossover}} \sim q E_f, \tag{3.6}$$

with E_f the Fermi energy.

This formula (3.6) then leads to the estimate $q = 0.2$, which is considerably smaller than the jellium value of $q = 0.5$ at the same density. The fact that both values are substantially different from the Fermi distribution with $q = 1$ testifies to strong electron–electron correlations, while the major difference from the jellium value shows the simultaneous importance of the electron–ion interaction.

All this is consistent with the discussion of condensed Na under normal conditions in sections 3.1 and 3.2, and naturally prompts the question as to whether chemical bonding can again be invoked to understand the behaviour of expanded fluid Cs along the liquid–vapour coexistence curve. That this is indeed so is strongly supported by the extensive ionic structural data on heavy alkalis. The neutron scattering experiments at high temperatures and pressures thereby required have been reviewed very recently by Winter and Bodensteiner [34], as well as by Winter and Hensel [35]. The former workers write "in comparison to the strong density dependence of the number of nearest neighbours, the distance of nearest neighbours remains almost constant during the expansion."

As partly anticipated by Warren and Mattheiss [36], a way forward is then given by studying the way in which the coordination number, z say, varies with density d along the coexistence curve. These authors employ a quasi-crystalline model of a liquid structure. Then, they point out that (a) the coordination number varies almost linearly with density d, and that (b) useful models are given by a body-centered cubic structure for $z = 8$ (see also the model by March and Tosi in section 3.2), simple cubic for $z = 6$, whereas for $z = 4$, they considered both simple tetragonal and diamond structures. Their data relating z and d, it turns out, when extrapolated linearly to the critical density of Cs, namely $d_c = 0.38$ g/cm^3, leads to a predicted coordination number near to $z = 2$. This will be argued below to motivate a model of the metal–insulator transition, but for the moment let us note that d_c at $z = 2$, plus the Warren–Mattheiss data [36] for z versus d, is fitted to better than 2% accuracy by

$$d_{\text{liquid}} = az + b, \tag{3.7}$$

where $a = 0.23$ and $b = -0.08$, both in g/cm^3.

At this stage, it will be helpful to return to the characterization of the condensed state of the alkalis in terms of diatoms, in view of the constancy of the near-neighbour "bond" distance along the Cs coexistence curve. Specifically, for Na eqs. (3.2) and (3.4), relevant to coordination numbers $z = 8$ and 6, respectively, lead to near-neighbour distances $r_{bcc} = 7.07$ a.u. (see table 1) and $r_{sc} = 6.82$ a.u., which are remarkably close bearing in mind the very different densities.

This characterization of crystalline Na in terms of a "bond" having length about a factor 1.2 larger than that of free-space Na_2 now prompts one to return to the result (3.7) for fluid Cs and to discuss its relation to the metal–insulator transition. First, in contemplating just how the two-component liquid metal built from Cs^+ and electrons e^- could eventually have a structure corresponding to $z = 2$, it is useful to refer to the classical counterpart of a mixture of charged hard spheres and neutralizing point ions studied by Gillan et al. [37]. Using Monte Carlo simulation, these workers demonstrated that for sufficiently strong coupling, polymerization can occur.

Returning to the quantum-mechanical case of a zig-zag chain of Cs ions, from Peierl's theorem one has (see also section 4) that there will be a bond length distortion, since a one-dimensional metal cannot exist. Here, then, is a mechanism for the metal–insulator transition: for this to occur in the present model, it is necessary that the coordination number of the ions should drop to a value near to $z = 2$. This seems plausible, since knowledge of Cs vapour demonstrates a mixture of neutral atoms and dimers.

To summarize, one can expect a considerable measure of short- to medium-range electronic spatial correlation in the valence electron assembly of the expanded fluid alkalis, and in particular in Cs. Eventually, the combination of electron–electron and electron–ion interactions will lead back to a low density vapour situation of monomers and dimers.

4. Can molecules exist in metallic phases?

The considerations presented above for normal and expanded alkali metals can leave little doubt that chemical arguments are very helpful in understanding the strongly correlated electronic behaviour in these materials.

This leads, rather naturally, to the question as to whether molecules can exist in ordered metallic phases, i.e. can molecular metallic crystals exist? To be specific, one has in mind the behaviour of insulating molecular crystals, such as are formed by H_2 and I_2 under normal conditions as pressure is applied at $T = 0$, to eventually lead to an insulator–metal transition. Will such metallic phases necessarily have no I_2 or H_2 molecules?

To address this question, it will be useful in section 4.1 to summarize the results of Ferraz et al. [38], using a model to simulate a hydrogen molecule embedded in jellium. Then, in section 4.2, some discussion of laboratory and computer experiments will be presented and brought into contact with the above model. Iodine will be considered in section 4.3, while bond-charge repulsion will be investigated in section 4.4.

4.1. HEITLER–LONDON THEORY OF H_2 WITH SCREENED COULOMB INTERACTIONS

To introduce this discussion of whether molecules can exist in metallic phases, e.g. metallic H_2, let us at this point summarize the results of a model of a single H_2 molcule. This model was set up by Ferraz et al. [38] to study when screening of the interactions in a Heitler–London theory of a single H_2 molecule would result in dissociation. On can think of such a procedure as a test of the instability of an electron gas against molecular bonding. Therefore, Ferraz at al. [38] replaced the bare interaction $1/r_{ij}$ by $\exp(-k_{TF}r_{ij})/r_{ij}$ in the usual free-space Heitler–London theory of H_2. The inverse screening length k_{TF} was taken to be given by the usual Thomas–Fermi result $k_{TF}^2 = 4k_f/\pi a_0$, where k_f is the Fermi wave number of the electron gas, related to the constant density ρ_0 in eq. (1.1) by $\rho_0 = k_f^3/3\pi^2$. The conclusion was that as the electron gas density was increased continuously, the binding energy of the molecule was eventually lost. Figures 4 and 5 illustrate this for two values of the screening length k_{TF}^{-1}.

4.2. METAL–INSULATOR TRANSITION IN HYDROGEN

Ferraz et al. [38] used the critical density at which the H_2 molecule dissociated as an, admittedly rough, measure of the molecular insulator–metallic hydrogen transition. However, at this point it must be stressed that, in analogy with solid I_2 to be discussed in section 4.3, there may well be metallization in solid hydrogen at a lower pressure than such a model predicts, due to energy gap closure in the originally insulating molecular H_2 phase. Such gap closure is a property of the order in the crystal, if not long-range then at least local coordination. It seems possible at the time of writing that in a limited pressure range, it may be that molecules can remain undissociated even after metallization has occurred.

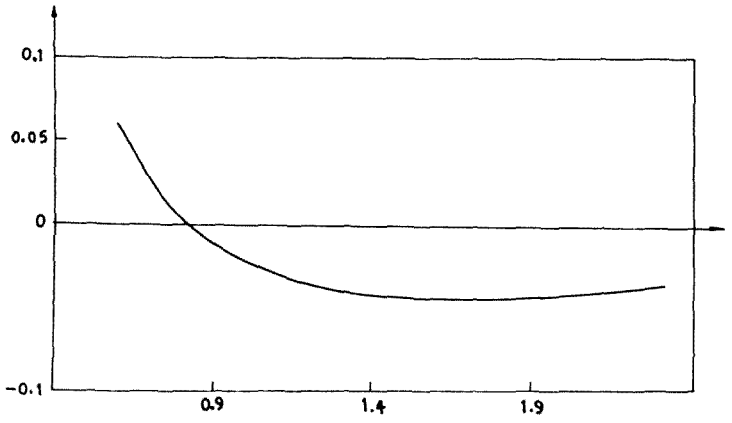

Fig. 4. Potential energy curve for Heitler–London model of an H_2 molecule using screened Coulomb interactions with an inverse Thomas–Fermi screening length $k_{TF} = 1$.

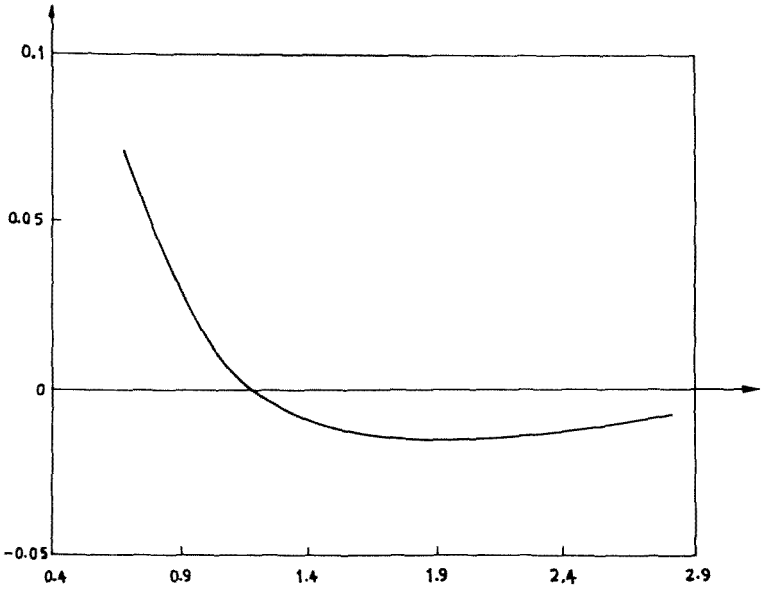

Fig. 5. Same as fig. 4, but with $k_{TF} = 1.1$.

It is relevant, however, to note here that the estimates of the critical density (r_s) value made by Ferraz et al. [38] agreed quite well with the report of Hawke et al. [39] that the transition to a metallic state of hydrogen with no molecules present has been observed experimentally. However, later authors (see the comments of Ross [40] and also those by Silvera [41]) have raised questions about this reported observation of the metal–insulator transition and the matter is not settled at this time. On the other hand, this is not a dispute that, under sufficiently high pressure, a metallic phase with no molecules present will be formed. Ross [40] estimates the pressure at which this

happens to be between 1 and 4 Mbar, and this is consistent with later and sharper estimates. Thus, based on measured equation of state extrapolation, Mao et al. [42] estimate 2.3 Mbar, whereas Van Straaten and Silvera [43] suggest a value of 2.8 Mbar after also invoking the Herzfeld criterion. Furthermore, the quantum computer simulation made by Ceperley and Alder [44] yields a transition to a cubic atomic phase at 3 Mbar.

It is worth adding here, in connection with these quantum Monte Carlo calculations by Ceperley and Alder [44], that these rest on few approximations which are in fact (1) the restriction to less than a few hundred atoms, (2) incomplete treatment of Fermi statistics, i.e. antisymmetry, and (3) the finite length of the Monte Carlo runs. The method also has some uncertainty with respect to the crystal structure of the molecular phase. However, these workers carried out calculations for several crystal structures, and their results indicated that the oriented Pa3 phase is preferred at densities higher than that corresponding to $r_s = 1.45a_0$. This orientation ordering transition has been placed close to 1 Mbar.

4.3. PROPERTIES OF COMPRESSED SOLID IODINE

Briefly, solid molecular iodine has a planar structure with the molecules lying in the planes. The interaction between the planes is weak as in graphite, and the crystal exhibits two-dimensional behaviour.

What is central for the present discussion is that electrical transport measurements by Drickamer and coworkers [45] have demonstrated that iodine becomes metallic under pressure. Specifically, the resistivity ρ, at low pressure, has the typical behaviour

$$\rho \sim \exp(\Delta/2k_B T) \tag{4.1}$$

of a semiconducting material. However, at pressures in excess of 160 kbar, the crystal was found to exhibit metallic conduction in the direction perpendicular to the planes, the temperature variation of ρ now having the form

$$\rho \sim T^{\alpha}; \quad \alpha > 0. \tag{4.2}$$

In contrast, a small residual energy gap remains parallel to the planes, with semiconducting behaviour as a consequence. Finally, as the pressure is increased beyond 220 kbar, the crystal shows metallic behaviour in all directions and has a smaller resistivity in the direction parallel to the planes.

Although there has been some controversy in the last decade as to the nature of the second transition at 220 kbar [46], from X-ray diffraction studies there can no longer be any doubt that iodine is still a molecular crystal after the first transition at 160 kbar. There is no structural change, but the relevant band gap goes continuously to zero as the pressure approaches that value [45]. Below 160 kbar, one has effectively two gaps: $\Delta_{\perp}$

and $\Delta_{||}$, which are related to conduction in directions perpendicular and parallel, respectively, to the planes. The first gap becomes zero at 160 kbar, while the second one closes at 220 kbar, giving rise to metallic conduction in the planes as well. In this third pressure range, the resistivity is smaller in the direction parallel to the planes, iodine exhibiting therefore anisotropic behaviour.

Siringo et al. [47] have carried out quantum-chemical calculations of the energy bands, including a full account of the variation of the structure of the nuclei with pressure from the experiments of Takemura et al. [48]. Their chemical treatment was based on a two-dimensional model of 5p-electron localization going back to Bersohn [49] who did not, of course, study the model under pressure at that time. Figure 6 shows a plot of the indirect energy band gap between the top of the valence

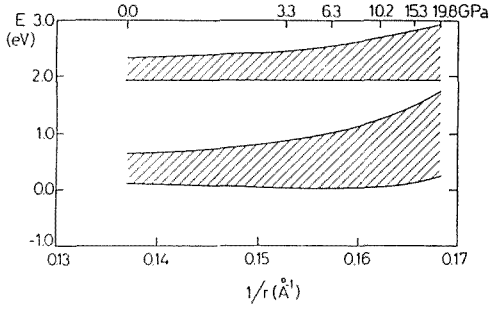

Fig. 6. Results of a two-dimensional band structure calculation of solid iodine [47], showing the reduction of the energy band gap with increasing pressure (top scale in GPa) and as a function of $1/r$ (lower scale in $Å^{-1}$), where r is the cube root of the unit-cell volume.

band and the bottom of the conduction band as a function of pressure. It is striking that the band gap reduces from its (fitted) value of 1.35 eV at zero pressure to 0.1 eV at ~200 kbar. Extrapolation suggests that such a two-dimensional structure will become metallic due to band overlap at ~230 kbar, in close accord with the experiments described above.

On the other hand, a complete description of solid iodine under pressure must incorporate the effects of the interaction between planes which are no longer negligible under high pressure. This problem has subsequently been tackled by Siringo et al. [50], again with good agreement with experiment. Thus, two band gaps are found, and calculating effective masses of electrons and holes from their energy band structure, the main features of the transport measurements by Drickamer and coworkers [45] can be understood in general terms.

Very recently, Pucci et al. [51] examined in some detail many-body effects in a model which turns out to be relevant to the above treatments of the molecular solids H_2 and I_2, and it is these latter aspects that will be summarized below.

4.4. ELECTRON–ELECTRON INTERACTIONS AND THE ROLE OF BOND-CHARGE REPULSION IN LOW-DIMENSIONAL SOLIDS

As is clear from the Wigner transition described in section 2, band overlap is only one of the possible mechanisms by which metal–insulator transitions can occur. Therefore, Pucci et al. [51] have given attention to the role played by the Peierls instability [52], already referred to in the discussion of expanded fluid Cs above, and the Coulomb interaction (especially bond-charge repulsion) at high pressure. To do this, these workers employed a model Hamiltonian, which will be briefly summarized below.

Model Hamiltonian

The model Hamiltonian employed is set up following the pioneering work of Su, Schrieffer and Heeger (SSH) [53]. Adding electron–electron interactions in accord with the work of Hubbard [54] gives the Hamiltonian $H = H_{SSH} + H_{ee}$, where

$$H_{SSH} = -\sum_{i,\sigma}[t_0 - \alpha(u_{i+1} - u_i)](C^+_{i+1,\sigma}C_{i,\sigma} + \text{h.c.}) + \tfrac{1}{2}K\sum_i (u_{i+1} - u_i)^2 + \sum_i \frac{P_i^2}{2M}\,, \tag{4.3}$$

$$H_{ee} = \frac{U}{2}\sum_{i,\sigma} n_{i,\sigma}n_{i,-\sigma} + V\sum_i n_i n_{i+1}\,, \tag{4.4}$$

where C_i^+ (C_i) creates (annihilates) an electron at site i, $n_{i,\sigma} = C^+_{i,\sigma}C_{i,\sigma}$, $n_i = \Sigma_\sigma n_{i,\sigma}$ and P_i is the momentum conjugated to the amplitude of the structural distortion u_i. t_0 is the transfer integral, U the on-site repulsion, and V the nearest-neighbour site repulsion.

By varying the relative magnitude of the parameters appearing in eqs. (4.3) and (4.4), one can have a rich variety of different physical behaviour [46].

Dimerization in systems such as *trans*-polyacetylene produces a charge-density wave (CDW) with wave vector $k = 2k_f$ (where k_f is the Fermi momentum), i.e. an inhomogeneous charge distribution. One could then expect that Coulomb interaction would oppose the dimerization and screen the $2k_f$ potential in such a way so as to reduce the single-particle gap. However, a number of model calculations have shown that weak interactions tend to enhance the dimerization [55–58].

Recently, Kivelson et al. [59] have considered the most general form of H_{ee} and have denoted with $V(n, m, l, p)$ the matrix element of the electron–electron interaction potential $V(r)$:

$$V(n,m,l,p) = \int \mathrm{d}r\,\mathrm{d}r'\rho_{np}(r)\rho_{ml}(r')V(r-r'), \tag{4.5}$$

where n, m, l, p are site indexes and ρ_{np} is the matrix element of the electron-density operator $\rho(r)$ in the Wannier representation. With this notation $U = 2V(0, 0, 0, 0)$,

$V = 2V(0, 1, 1, 0)$, the bond charge repulsion is $W = 2V(0, 1, 0, 1)$, and the cross coupling term between the bond and side charge densities is $X = 2V(0, 1, 1, 1)$.

By considering the continuum limit of the complete Hamiltonian, Kivelson et al. [59] have suggested that W might tend to suppress dimerization under the condition

$$3W > V. \tag{4.6}$$

While it may well be that the conclusions of Kivelson et al. [59] do depend strongly on the use of a δ-function interaction [46], Pucci et al. [51] have argued that their assumptions do indeed become more appropriate under pressures sufficiently high to markedly increase the screening of the interaction. To demonstrate this, they have calculated [51] W together with V and the on-site repulsion U as a function of interatomic separation by using a Gaussian approximation to the electron–electron interaction potential, with parametrization appropriate to iodine and hydrogen.

The terms relevant to the study of Coulomb dimerization effects are (1) the first-order energy $(3W - V)$ (compare the inequality (4.6)), and (2) the second-order contribution $U^2/2t_0$ (see, for instance, ref. [56]). In fig. 7, the results of these calculations [51]

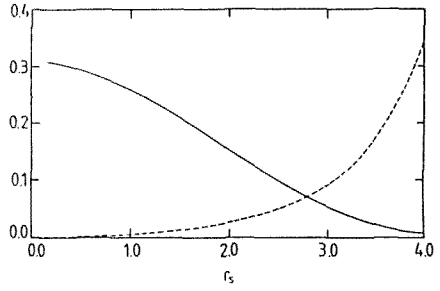

Fig. 7. First-order dimensionless ratio $(3W - V)/U$ (solid line) and second-order term $U/2t_0$ (dashed line) versus mean site separation for iodine. The same plots for hydrogen have similar shapes, but curves now cross at $r_s = 0.8$ compared with $r_s = 2.8$ for iodine in the figure.

for $(3W - V)/U$ and $U/2t_0$ as a function of the dimensionless density parameter r_s are displayed. It is seen that $(3W - V)/U$ is positive and greater than $U/2t_0$ at high densities. (The crossover point in fig. 7 is $r_s \sim 2.8$ for I: for H, it is $r_s \sim 0.8$ [51].) One might argue that the disappearance of the dimerization is heralding the onset of the monatomic phase (compare sections 4.1 and 4.2).

Of course, it must be stressed that one has not only to show that $3W - V > 0$ but also that this positive contribution overcomes the negative contribution derived from $U^2/2t_0$. In the Hartree–Fock approximation, which is valid [56] for small values of U and for $y = (2\alpha/t_0)u_0 < 0.2$, it has been shown [51], for the half-filled band case $(X = 0)$, that when

$$\frac{3W - V}{U} > 0.27 \frac{U}{2t_0}, \tag{4.7}$$

Coulomb repulsion opposes dimerization.

One has to be careful in necessarily accepting the quantitative validity of a one-dimensional model for solid H_2 and I_2. One notes also that the model does not include the cross-coupling term X between the bond and side charge densities. This term is larger than V and W in the extreme screening limit [59] and could increase the pressure at which the onset of the monatomic phase occurs. However, the above-mentioned results, where comparison is possible, are in qualitative agreement with the work of Wu et al. [61], who start from the full Coulomb interaction, with general strength and range.

5. Discussion and summary

Both analytic theory and Monte Carlo computer simulation agree that as the density of the jellium model is lowered, the electronic momentum distribution $n(p)$ exhibits in the metallic phase a reduction in the discontinuity at the Fermi momentum p_f, and that this discontinuity q eventually tends (most probably discontinuously) to zero as one passes through the metal–insulator (Wigner) transition to a localized electron crystalline phase.

Although for some purposes this model is useful for the so-called "nearly-free electron" metals Na and K, from existing studies on the Heisenberg model it is next shown that a picture of strongly correlated electrons can explain a number of important properties. Although such behaviour is, as yet, difficult to demonstrate experimentally in the crystalline phase, diffraction experiments on liquid Na and K exhibit directional bonding effects which are usefully described in terms of s–p hybridization combined with resonance à la Pauling. To attempt to understand the alkali metals as the density is lowered and the electronic correlation becomes increasingly important, magnetic susceptibility data on expanded fluid Cs has been analyzed by Chapman and the present author, using heavy fermion theory. Their conclusions are related to (a) the predictions from the jellium model of the discontinuity q in the electron momentum distribution, and (b) the possibility of directional bonding. Again, it seems that the combination of strong electron–electron correlation with significant electron–ion interaction is usefully represented by a chemical type of picture, even though one is still in the metallic phase.

While the above systems are truly three-dimensional, some discussion has also been given of solid iodine near the metal–insulator transition. This system is quasi two-dimensional and evidence is presented, both experimental and theoretical, for the existence of a metallic phase under pressure in which, at least over a limited range of pressure, there is a coexistence of I_2 molecules and the metallic state. The possibility that solid hydrogen may have a region of similar behaviour is finally considered, together with some discussion of the way in which electron correlation is again important in the behaviour of the metallic state as the pressure is varied.

Appendix

Relation between different model representations of the ground-state energy of metal structures

The purpose of this appendix is to compare and contrast three apparently different representations (denoted I–III below) of the ground-state energy E of metal structures. As will be seen, only method I takes explicit account of the Fermi surface which still exists in the metallic phase near the metal–insulator transition.

I. INTERACTION ENERGY BETWEEN LINEARLY SCREENED METAL IONS

The conventional representation of the ground-state energy E of an s–p metal is to write for a specified configuration $\{\boldsymbol{R}_i\}$ of the ions:

$$E(\{\boldsymbol{R}_i\}) = E(V) + \sum_{i<j} \phi(|\boldsymbol{R}_i - \boldsymbol{R}_j|, V), \tag{A1}$$

where both parts of the decomposition (A1) depend on volume, but only the second on structure. The basis of such a representation is afforded, for point ions in a high density electron liquid, by the second-order perturbation treatment given in the appendix of the paper by Corless and March [62,63]. An illustration of the way in which the pair potential ϕ depends on volume is its asymptotic form for large r, which is proportional to $\cos(2k_f r)/r^3$, due to the assumed spherical, and sharp Fermi surface of diameter $2k_f$. This behaviour can be compared qualitatively with that of $g(r)$ for electrons in jellium in the metallic phase (see section 2). The way in which the Fermi surface shape affects the asymptotic behaviour is discussed in ref. [64].

II. HEISENBERG REPRESENTATION USING DIATOM PROPERTIES

In the main text, the representation of $E(\{\boldsymbol{R}_i\})$ for a specified crystal structure was summarized, using the Heisenberg Hamiltonian. Following Poshusta and Klein [25], this was characterized by potential energy curves of appropriate states of the diatom.

III. ANALYSIS OF METAL-THEORY ENERGY AS A FUNCTION OF LATTICE SPACING IN TERMS OF DENSITY-INDEPENDENT PAIR POTENTIAL

Carlsson et al. [65] and Esposito et al. [66] proposed another method, based on the calculation of the ground-state energy E for a specified crystal structure as a function of the lattice parameter by the standard methods of the electron theory of metals. Given this energy for all values of the lattice parameter, these workers show how a unique, density-independent pair potential could be extracted. Their method will be summarized below; it is, of course, to be expected that such a density-independent pair potential will be different for each crystal structure considered. Carlsson et al. [65] displayed this pair potential for K (bcc) and Cu (fcc), as well as for a transition metal.

It seems clear that there must be an intimate relationship between methods II and III even though, as mentioned above, Carlsson et al. calculated E for, say, fcc Cu metal by the standard procedures of the electron theory of metals. Although this is in obvious contrast to the use of diatoms by Malrieu et al. [21], it will now be noted that the mode of extraction of a pair potential – to be summarized below – can in fact be applied to the quantum-chemical approach.

Carlsson et al. write, with near-neighbour separation r,

$$E(r) = \tfrac{1}{2} \sum_p n_p \, \phi(s_p r), \tag{A2}$$

where ϕ is the (assumed) volume-independent pair potential. In eq. (A2), the sum is over spherical shells p containing n_p atoms at a distance $R_p = s_p r$ from the atom at the origin. Evidently, s_p is the dimensionless ratio of the pth-neighbour distance to the near-neighbour separation.

Carlsson et al. then show that, given E as a function of near-neighbour separation r, eq. (A2) can be inverted to find the pair potential. Their result is:

$$\phi(r) = \frac{2}{n_1} E\left(\frac{r}{s_1}\right) - \sum_{p=2}^{\infty} \left(\frac{2}{n_1}\right)\left(\frac{n_p}{2}\right)\left(\frac{2}{n_1}\right) E\left(\frac{s_p r}{s_1^2}\right)$$

$$+ \sum_{p,q=2}^{\infty} \left(\frac{2}{n_1}\right)\left(\frac{n_p}{2}\right)\left(\frac{2}{n_1}\right)\left(\frac{n_q}{2}\right)\left(\frac{2}{n_1}\right) E\left(\frac{s_p s_q r}{s_1^3}\right) - \ldots \, . \tag{A3}$$

In view of the utility of the Heisenberg model for Na, as discussed in section 3, it would clearly be of interest to connect the quantum-chemical potential energy curves entering, say, eqs. (3.2) and (3.3) with the metal-physics pair potential (actually given for K rather than Na) by Carlsson et al. [65].

The connection of methods II and III with method I is less clear-cut, although also plainly of interest. The point to be emphasized, in concluding this appendix, is that methods II and III do not have included within them the metal–insulator transition in monovalent metals like the alkalis as the near-neighbour distance is increased sufficiently. Although approaches II and III can still have merit for the total energy as a function of r, they do not reflect the discontinuity q at the Fermi surface in the metallic phase as a function of near-neighbour distance. To illustrate the consequences of this, consider the example of jellium already discussed at length in section 2. There, the virial theorem [7] relating total energy E, kinetic energy T and potential energy U reads

$$2T + U = -r_s \frac{\mathrm{d}E}{\mathrm{d}r_s} , \tag{A4}$$

which can be used to show that at the Wigner electron liquid–electron crystal transition (therefore first order), $\mathrm{d}E/\mathrm{d}r_s$ discontinuous implies that $T(r_s)$ and $U(r_s)$ are separately

discontinuous at the metal–insulator transition, although the sum $E = T + U$ is continuous across the transition. One expects a related situation in the expanded alkalis in crystalline phases as a function of near-neighbour separation, and clearly the assumption underlying methods II and III is that such discontinuities are not important quantitatively in these cases. More work is clearly needed on this point before one can take this assumption as well established, although it seems quite plausible.

References

[1] C.A. Coulson and I. Fischer, Phil. Mag. 40(1949)386.
[2] M.C. Gutzwiller, Phys. Rev. A137(1965)1726.
[3] E.P. Wigner, Phys. Rev. 46(1934)1002; Trans. Faraday Soc. 34(1938)678.
[4] K.S. Singwi and M.P. Tosi, in: *Solid State Physics*, Vol. 36, ed. H. Ehrenreich, F. Seitz and D. Turnbull (Academic Press, New York, 1981), p. 177.
[5] D.M. Ceperley and B.J. Alder, Phys. Rev. Lett. 45(1980)566.
[6] F. Herman and N.H. March, Sol. Stat. Commun. 50(1984)725.
[7] N.H. March, Phys. Rev. 110(1958)604.
[8] N.H. March, M. Suzuki and M. Parrinello, Phys. Rev. B19(1979)2027.
[9] E.P. Wigner and F. Seitz, Phys. Rev. 43(1933)804.
[10] T. Gaskell, W. Jones and N.H. March, Phys. Lett. 23(1966)673.
[11] A. Holas and N.H. March, Phys. Chem. Liquids 17(1987)215.
[12] N.H. March, Phys. Lett. A108(1985)368.
[13] N.H. March and M.P. Tosi, *Coulomb Liquids* (Academic Press, New York, 1986).
[14] K.A. Dawson and N.H. March, Phys. Chem. Liquids 14(1984)131.
[15] A. Schinner, Phys. Chem. Liquids 18(1988)117.
[16] A.B. Bhatia and N.H. March, Phys. Chem. Liquids 13(1984)313.
[17] J.C. Kimball, J. Phys. A8(1975)1513.
[18] N.H. March, J. Phys. A8(1975)L133.
[19] E. Daniel and S.H. Vosko, Phys. Rev. 120(1960)2041.
[20] N.H. March and W.H. Young, Phil. Mag. 4(1959)384.
[21] J.P. Malrieu, D. Maynau and J.P. Daudey, Phys. Rev. B30(1984)1817.
[22] P.A. Egelstaff, N.H. March and N.C. McGill, Can. J. Phys. 52(1974)1651.
[23] P.J. Dobson, J. Phys. C11(1978)L295.
[24] M.W. Johnson, private communication and to be published (1990).
[25] R.D. Poshusta and D.J. Klein, Phys. Rev. Lett. 48(1982)1555.
[26] J. Chihara, J. Phys. F17(1987)295.
[27] S. Tamaki, Can. J. Phys. 65(1987)286.
[28] N.H. March and M.P. Tosi, Phys. Chem. Liquids 10(1980)113.
[29] R.G. Chapman and N.H. March, Phys. Rev. B38(1988)792.
[30] W. Freyland, Phys. Rev. B20(1979)5104.
[31] W.W. Warren, Phys. Rev. B29(1984)7012.
[32] T.M. Rice, K. Ueda, H.R. Ott and H. Rudigier, Phys. Rev. B31(1985)594.
[33] L. Pauling, Proc. Nat. Acad. Sci. 39(1953)551.
[34] R. Winter and T. Bodensteiner, High Pressure Res. 1(1988)23.
[35] R. Winter and F. Hensel, Phys. Chem. Liquids (1989), in press.
[36] W.W. Warren and L.F. Mattheiss, Phys. Rev. B30(1984)3103.
[37] M.J. Gillan, B. Larsen, M.P. Tosi and N.H. March, J. Phys. C9(1976)889.
[38] A. Ferraz, F. Flores and N.H. March, J. Phys. Chem. Sol. 45(1984)627.

[39] P.S. Hawke, T.J. Burgess, D.E. Duerre, J.G. Huebel, R.N. Keeler, H. Klapper and W.C. Wallace, Phys. Rev. Lett. 41(1978)994.
[40] M. Ross, Rep. Prog. Phys. 48(1985)1.
[41] I.F. Silvera, private communication and to be published.
[42] H.K. Mao, A.P. Jephcoat, R.J. Hemley, L.W. Finger, C.S. Zha, R.M. Hazen and D.E. Cox, Science 239(1988)1131.
[43] J. Van Straaten and I.F. Silvera, Phys. Rev. B37(1988)1989; Phys. Rev. B, in press.
[44] D.M. Ceperley and B.J. Alder, Phys. Rev. B36(1987)2092.
[45] H.G. Drickamer, Sol. Stat. Phys. 17(1965)1; H.G. Drickamer, R.W. Lynch, R.L. Clendenen and E.A. Perez-Albuerne, Sol. Stat. Phys. 19(1966)135.
[46] See, for example, the review by F. Siringo, R. Pucci and N.H. March, High Pressure Res., to appear.
[47] F. Siringo, R. Pucci and N.H. March, Phys. Rev. B37(1988)2491.
[48] K. Takemura, Y. Fujii, S. Minomura and O. Shimomura, Sol. Stat. Commun. 30(1979)137; for later refs., see [46].
[49] R. Bersohn, J. Chem. Phys. 36(1962)3445.
[50] F. Siringo, R. Pucci and N.H. March, Phys. Rev. B38(1988)9567.
[51] R. Pucci, F. Siringo and N.H. March, Phys. Rev. B38(1988)9517.
[52] R.E. Peierls, *Quantum Theory of Solids* (Oxford University Press, 1955).
[53] W.P. Su, J.R. Schrieffer and A.J. Heeger, Phys. Rev. Lett. 42(1979)1698.
[54] J. Hubbard, Proc. Roy. Soc. A276(1963)238.
[55] P. Horsch, Phys. Rev. B24(1981)7351.
[56] S. Kivelson and D.E. Heim, Phys. Rev. B26(1982)4278.
[57] J.E. Hirsch and M. Grabowksi, Phys. Rev. Lett. 52(1984)1713.
[58] D.K. Campbell, T.A. DeGrand and S. Mazumdar, Phys. Rev. Lett. 52(1984)1717.
[59] S. Kivelson, W.P. Su, J.R. Schrieffer and A.J. Heeger, Phys. Rev. Lett. 58(1987)1899.
[60] H. Takayama, Y.R. Lin-Liu and K. Maki, Phys. Rev. B21(1980)2388.
[61] C. Wu, X. Sun and K. Nasu, Phys. Rev. Lett. 59(1987)831.
[62] G.K. Corless and N.H. March, Phil. Mag. 6(1961)1285.
[63] See also, for example, the review by J.M. Ziman, Adv. Phys. 13(1964)89.
[64] F. Flores, N.H. March, Y. Ohmura and A.M. Stoneham, J. Phys. Chem. Sol. 40(1979)531.
[65] A.E. Carlsson, C.D. Gelatt and H. Ehrenreich, Phil. Mag. A41(1980)241.
[66] E. Esposito, A.E. Carlsson, D.D. Ling, H. Ehrenreich and C.D. Gelatt, Phil. Mag. A41(1980)251.